Proceedings of the
International Conference on Mechanical Engineering 2003
(ICME2003) 26- 28 December 2003, Dhaka, Bangladesh

ICME03-AM-09

Parametric study of the Sheet Metal Forming Processes using Adaptive Refinement Techniques

Mohd. Ahmed[1]*, G.S. Sekhon[1], Devender Singh[2]

[1]Deptt. of Applied Mechanics, IITDelhi, New Delhi-110016,India
*Corresponding auther, e-mail: ahmed1md_69@hotmail.com
[2]All India Radio, Prasar Bharati, Bombay, India

ABSTRACT

In the present study, the influence of an important process parameter of the sheet metal forming processes, namely thickness of blank, has been analyzed using adaptive mesh refinement. In an adaptive technique, the mesh is automatically refined in areas of insufficient accuracy and in areas of sharp strain gradients. A recovery type error estimator based on the energy norm is used for guiding the h-refinement. Illustrative examples of sheet stretching operations are simulated. The refined meshes at different stages of deformation and CPU times are studied.

Keywords: Process Parameters, Adaptive Mesh refinement, Recovery procedures.

1. INTRODUCTION

The finite element method has found applications in the solution of a variety of problems. Among these is the analysis of different sheet metal forming operations. An area of concern is the possible error in the numerical solution of a given problem. The reliability of finite element analysis results can be enhanced through error estimation and adaptive procedures. The goal of all adaptive techniques is to obtain numerical solutions efficiently and economically, i.e. restricting the discretization error within permissible limit at minimum computational cost. Contributions to the non-adaptive finite element analysis of sheet metal forming processes include those of, among others, Cao and Teodocia [1], Damir [2] and Mark and Julu [3]. Presently considerable research effort is underway for devising error estimators and adaptive mesh refinement procedures. Among the post processing type error estimators, one proposed by Zienkiewicz-Zhu [4] is perhaps most popular. It relies upon the so-called "recovery" of a higher order approximation of the computed variable of interest. The recovery of post processed stress field by the least squares method had been proposed by Zienkiewicz-Zhu [5]. More recently, a velocity based recovery technique has been presented by Singh et al [6]. A mesh regularization method has been proposed by Yoon and Huh [7] for the enhancement of the efficiency in sheet metal forming analysis. The present investigation deals with the study of adaptive mesh refinement during parametric study of the sheet stretching operation. The parameter of interest is namely, the blank thickness.

2. FINITE ELEMENT FORMULATION

The weak formulation of a boundary value problem can be obtained by using the principle of virtual work along with a penalty method to enforce incompressibility. It can be expressed by the following equation [8].

$$\int_{\Omega} \bar{\sigma}\, \delta\dot{\bar{\varepsilon}}_i \, d\Omega + K \int_{\Omega} \varepsilon_V \, \delta\dot{\varepsilon}_i \, d\Omega - \int_{S_3} \tau\, \delta v_i \, d\Gamma_f = 0 \quad (1)$$

The equivalent stress and equivalent strain rate in Eq. (1) are defined as below.

$$\bar{\sigma} = \left(\tfrac{3}{2}\sigma'_{ij}\sigma'_{ij}\right)^{1/2}$$

$$\bar{\varepsilon} = \left(\tfrac{2}{3}\dot{\varepsilon}_{ij}\dot{\varepsilon}_{ij}\right)^{1/2} \quad (2)$$

The relevant interpolation equations can be written as follows.

$$x(\xi,\eta) = N(\xi,\eta)\,.\,x \text{ and } v(\xi,\eta) = N(\xi,\eta)\,.\,v \quad (3)$$

$$\dot{\boldsymbol{\varepsilon}} = \mathbf{B}\,.\,\mathbf{v} \quad (4)$$

If Eq. (4) is substituted in Eq. (1) and the Galerkin method is used to carry out integration, the following discrete system of equations is obtained.

$$\mathbf{G}(\mathbf{v}) = 0 \quad (5)$$

The system equations are obtained from elemental equations through an assembly procedure. The solution of Eq. (5) yields the global velocity vector. The solution may be carried out iteratively using Newton-Raphson method with linear line search technique.

3. THE ZZ ERROR ESTIMATION

For an approximate solution of the problem obtained by finite element solution, the error in the computed stress or displacement (velocity), e_σ^*, e_u^* is defined as the difference between the exact solution of stress or displacement (velocity), σ, u and the corresponding computed values, σ^h, u^h i.e.

$$e_\sigma^* = \sigma - \sigma^h$$
$$e_u^* = u - u^h \qquad (6)$$

The error can be evaluated in some appropriate norm. Since the finite element solution minimizes the error in the energy norm, the magnitude of the error in energy norm is a good measure of the overall quality of approximation. The integral measure of the error in energy norm is defined as below.

$$\|e\| = \left(\int_\Omega e_\sigma^{*T} D\, e_\sigma^* d\Omega \right)^{1/2} \qquad (7)$$

The relative error in energy norm, η, is defined as follows.

$$\eta = \frac{\|e\|}{\|u\|} \text{ x } 100 \quad \text{percent} \qquad (8)$$

In the above expression, $\|u\|$ is estimated from computed value of σ^h by using the following equations.

$$\|\bar{u}\|^2 = \|u^h\|^2 + \|e\|^2 \qquad (9)$$

where $$\|u^h\|^2 = \left[\sum_{i=1}^{ne} \|u^h\|_i^2 \right]$$

The finite element formulation for a metal forming problem is of the mixed type in which incompressibility is ensured by means of a penalty constant. It is, therefore, convenient to concentrate on the energy norm of the deviotoric part of the stress tensor only. The error norm, $\|e\|$ can be obtained by replacing the exact stresses in Eq. (7) by some recovered smooth stresses, σ^h, i.e.

$$\|e\|^2 = \int_\Omega (\sigma^{*/} - \sigma^{/h})^T (2\mu)^{-1} (\sigma^{*/} - \sigma^{/h})\ d\Omega \qquad (10)$$

4. ADAPTIVE MESH REFINEMENT STRATEGY

Various criteria can be used to assess the accuracy of an analysis. The appropriate refinement strategy will depend on the nature of the accuracy criterion that is to be satisfied. A very common requirement is to specify the achievement of a certain minimum percentage error in the energy norm.

The global error estimate may be defined as follows.

$$\|e\|^2 = \sum_{i=1}^{N} \|e_i\|^2 \qquad (11)$$

The error in individual elements in relation to the global error helps us to decide which portions of the mesh need improvement. Following are the techniques to carry out these improvements

(a) r-refinement i.e. relocating the position of nodes within the mesh
(b) h-refinement i.e. subdividing selected elements into smaller elements of the same type.
(c) p-refinement i.e. increasing the order of the interpolating polynomial of selected elements

Among the above techniques, h-refinement is the most generally employed.

5. PROPOSED MODEL

The problem of finite element modelling of axisymmetric sheet stretching operations is studied in the present work. The blank material is assumed as rigid-visco plastic or rigid-plastic. The elastic components of strain and strain rates are neglected. The punch and die are considered as rigid. Friction is present at the punch-blank and die-blank interface. The downward velocity of the punch can be arbitrarily specified.

The stress-strain relation of the material of the blank is assumed to be given the following relation.

$$\bar{\sigma} = (1 + a\,\bar{\varepsilon})\ \dot{\bar{\varepsilon}}^m \qquad (12)$$

Quantitative assessment of the error of the computed solution and adaptive mesh improvement to achieve the target accuracy are carried out. The energy norm of the error is adopted for assessing of the quality of the solution [9] and h-refinement scheme is employed for improving the mesh [5].

6. ILLUSTRATIVE EXAMPLES

The two-dimensional computer code **Adsheet2** developed in-house at IIT Delhi was used to simulate the axisymmetric sheet forming processes, schematically shown in Fig. (1). Recovery based adaptive finite element procedures have been implemented in the above code. The blank is discretized using six noded triangular elements. The input parameters were as follows.

Radius of punch R_p = 50.8mm,
Clamped radius of blank R_b = 59.18mm,
Die corner radius R_d = 6.35mm,
Velocity of Punch V_b = 1mm/sec,
Target error = 8%
Stress-strain relation [10]

$$\bar{\sigma} = 589[0.0001 + \bar{\varepsilon}]^{0.216} \qquad (13)$$

Owing to symmetry, only one half of the blank was modelled. For discussion purpose, the half sheet blank is divided into three regions. Region I is the portion of the blank between centre of blank and a point up to which the punch is in contact with the blank, region II corresponds to the portion of the blank neither in contact with punch nor with the die or blank holder, and region III corresponds to the portion of the blank which is in contact with the die and the blank holder.

6.1 Mesh

Three cases of sheet thickness namely, 1mm, 2mm and 3mm were considered. The initial mesh in each case was uniform such that for sheet of 1mm, 2mm and 3mm thickness, the total number of degrees of freedom were 2910, 3770 and 3382 respectively (Fig. 2). For 1mm sheet thickness, only a single remeshing was needed to manage the solution error through the total deformation process. However, two remeshings were required for the cases of 2mm and 3mm thick blank. The refined mesh for 1mm sheet thickness consisted of 1395 elements and 6340 degrees of freedom at a punch displacement of 2.5mm. Since only single remeshing occurred, the refined meshes remain same throughout subsequent stages. In the first remeshing for 2mm thick sheet, the number of elements and degrees of freedom were found to increase to 1239 and 5484 respectively. In the next remeshing, the number of elements and degrees of freedom decreased somewhat to 1031 and 4524 respectively. The number of elements and degrees of freedom in the refined mesh for a thickness of 3mm were 1444 and 6230 respectively at a punch displacement of 2.5mm. The corresponding values at punch displacement of 25.0mm were 1195 and 5168 respectively. The actual CPU times for adaptive analysis were 8 hours 15 minute, 7 hours and 6 hours 30 minute respectively for sheet thickness of 1mm, 2mm and 3mm.

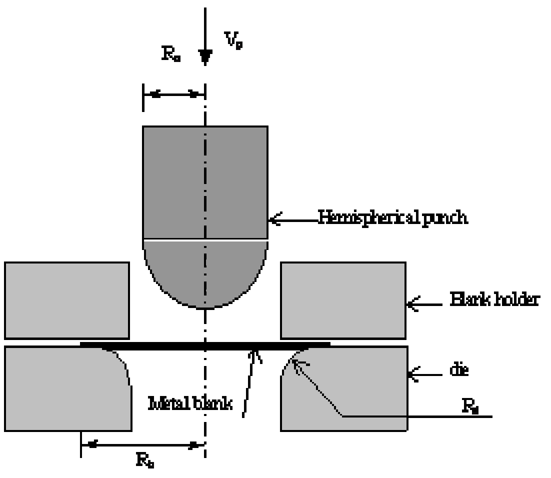

Fig. 1 Schematic Diagram of Sheet Forming

The computed mesh and deformed shapes at punch displacement of 2.5mm and 25.0mm for 1 mm thick sheet are shown in Fig. (3). From the mesh plots, it can be observed that after adaptive remeshing, the mesh becomes finer only in regions of high strain gradients and it becomes coarser in regions of low strain gradient. At a punch displacement of 2.5mm, a highly dense mesh is generated in region I except at the centre of blank, which has coarse mesh. Region II has high density of elements at the ends adjoining region I and region III. In the remaining portion of Region II, half has coarse mesh and half has finer mesh. The region III has a band of finer elements throughout its thickness around its outer periphery and coarser elements in the remainder. The corresponding mesh at 25.0mm punch displacement exhibits a similar trend of element distribution in different regions.

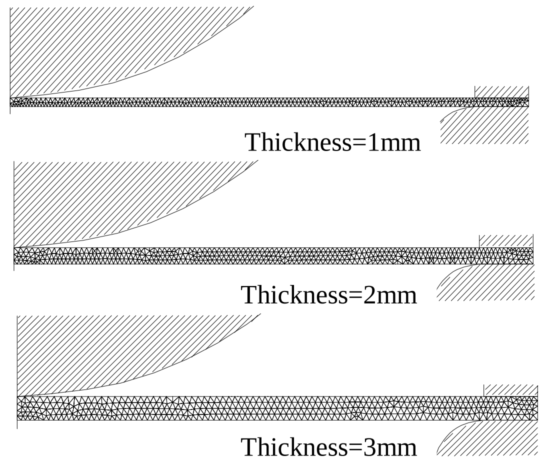

Fig.2 Undeformed mesh at different thicknesses of blank

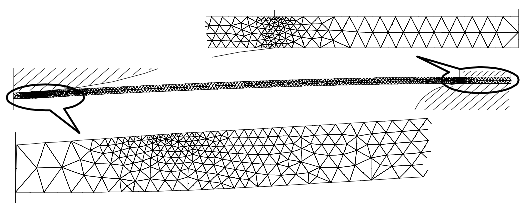

Fig. 3(i) Deformed mesh at punch travel of 2.5mm (Thickness=1.0mm)

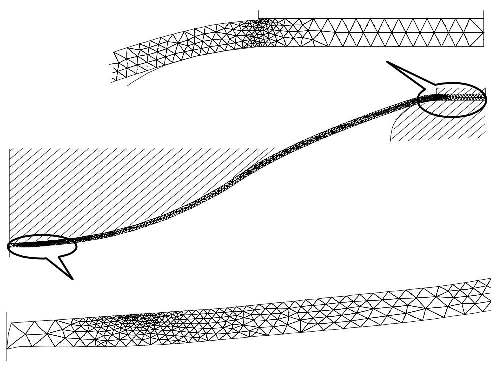

Fig.3 (ii)Deformed mesh at punch travel of 25mm (Thickness=1.0mm)

The element distribution corresponding to sheet thickness of 2mm and punch displacement of 2.5mm shows that the density of elements in region I and region III is high. In region I, the element density is highest at the punch-blank interface i.e. at the top surface of the sheet and it goes on decreasing towards the bottom of the sheet. The element density decreases along the radius too. The mesh in region II is more or less uniform but its density is smaller. Region III has a band of finer elements throughout its thickness. At punch travel of 25.0mm, the deformed mesh given in Figure 4 indicates that though regions I and region III, continue to have greater number of fine elements but their distribution is significantly altered. Region I, which is localized at punch travel of 2.5mm, becomes dispersed and the element density tends to decrease towards region II. In region III also, two distinct bands of fine elements develop. The mesh in region II becomes coarser with increase of punch travel.

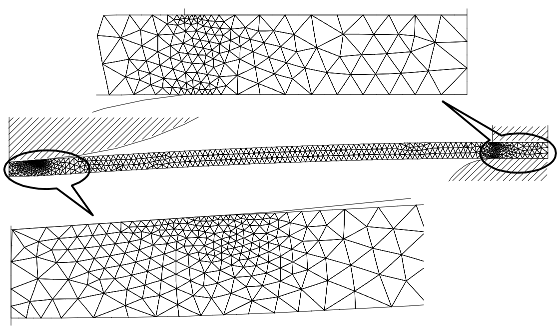

Fig. 4 (i) Deformed mesh at punch travel of 2.5mm (Thickness=2.0mm)

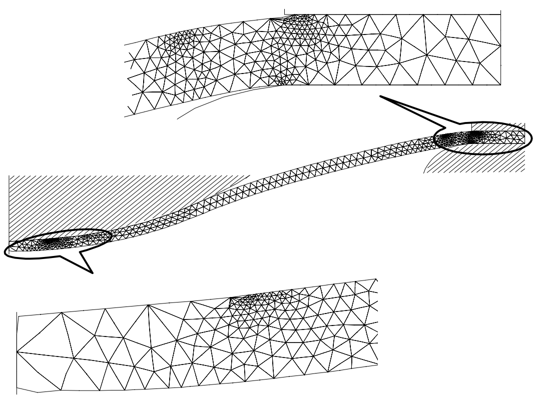

Fig.4 (ii) Deformed mesh at punch travel of 25mm (Thickness=2.0mm)

The mesh obtained at a punch displacement of 2.5mm for 3mm thick sheet shows that the density of elements in region I is high. The mesh in region II is composed of, more or less, uniform coarse elements except at the junction of regions I and II. Region III has a band of fine elements throughout its thickness. The elements density of the band decreases towards the middle of the sheet. The deformed mesh at punch travel of 25.0mm indicates that though regions I and region III, continue to have greater number of fine elements but their distribution is significantly altered. In region I, the zone of very high-density elements reduces in size. In region III also, bands of fine elements, which is spread throughout the sheet thickness at punch travel of 2.5mm becomes partitioned into two. The mesh in region II becomes coarser in the middle portion and finer at ends with increase of punch displacement.

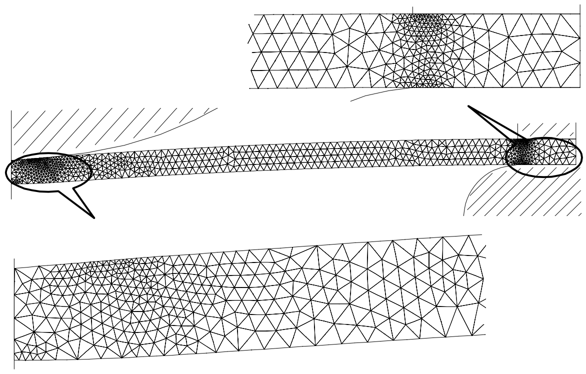

Fig. 5 (i) Deformed mesh at punch travel of 2.5mm (Thickness=3.0mm)

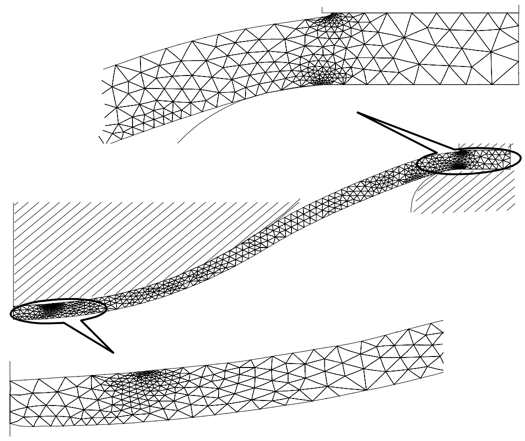

Fig.5 (ii) Deformed mesh at punch travel of 25mm (Thickness=3.0mm)

6.2 Punch Load

Figure (6) depicts the evolution of punch load at various stages of deformation in different cases of blank thickness. It is observed that the punch load as expected increases with increase of punch displacement and also with the increase of thickness of sheet. The increase of punch load in early stages of displacement is less as compared to the latter stages of displacement. The magnitudes of punch load at final punch displacement are 14.7kN, 35.1kN and 54.5kN for 1mm, 2mm and 3mm sheet thickness respectively.

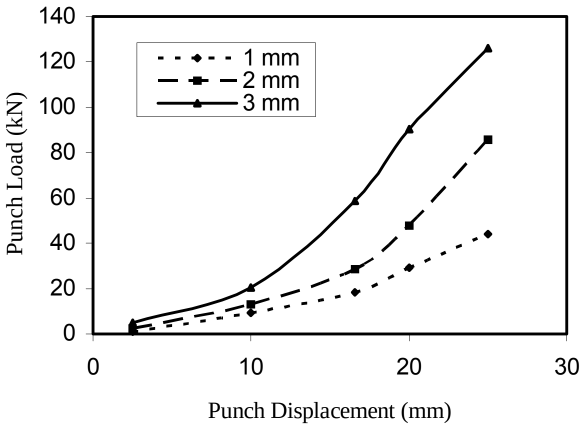

Fig.6 Punch Load – Punch Displacement curves for different thickness of blank

6.3 Effective strain

Table (1) lists the peak values of effective strain at different stages of deformation corresponding to different thicknesses of blank. It is inferred from the table that the magnitude of effective strain increases with increase of punch displacement. For example, the peak values of effective strain at punch displacements of 2.5mm and 25.0mm are 0.424725 and 0.952632 respectively for 1mm sheet thickness. The peak effective strain values for 1mm thickness of blank are smaller than those corresponding to 2mm and 3mm thickness of blank. But the comparison of peak effective strain values for 2mm and 3mm sheet thickness shows that the values corresponding to 2mm thickness are lower at initial stages of deformation but become higher with increase of deformation. For example, the peak values of effective strain at punch displacement of 2.5mm and 25.0mm are 0.426031 and 2.945496, and 0.447645 and 1.593838 respectively for 2mm and 3mm thickness of sheet.

Table 1: Peak values of effective strain ($\bar{\varepsilon}$) at different stages of deformation

Punch Travel (mm)	**Effective Strain** ($\bar{\varepsilon}$)		
	h = 1mm	**h = 2mm**	**h = 3mm**
2.5	0.424725	0.426031	0.447645
10.0	0.492764	1.996043	0.581243
15.0	0.616395	2.001042	0.796711
20.0	0.772430	2.006001	1.073174
25.0	0.952632	2.945496	1.593838

7. DISCUSSION OF THE RESULTS

The validity of the proposed model was verified by comparing the predictions of the forming load with those available in literature [10]. A good agreement is found between the two.

The influence of an important process parameter of sheet stretching namely thickness was studied through adaptive finite element simulation that efficiently captures high stress/strain gradient zones. Such zones are automatically refined to minimize the error in the solution. An initially uniform mesh becomes non-uniform after mesh refinement. The sheet of thickness 1mm requires only single remeshing but two remeshings were needed for 2mm and 3mm thick sheet to bring the error below the prescribed error limit of 8%. In the first remeshing, the number of elements got increased but with second remeshing, the numbers of elements become fewer. The elements in some regions of the blank become very fine after remeshing. It was observed that finer elements occurred in the same regions of the blank in all cases of sheet thickness. However, the distribution of elements is somewhat different. The finer element zone is wider in case of lower thickness of sheet but becomes localized with increase of blank thickness. Bands of high element density got developed at higher thickness of blank in these regions. The middle region has higher uniformity of element than that during the early stage of deformation. During later stages of deformation, mesh in this region has a mix of fine and coarse elements. The simulation time decreases with increase of sheet thickness. The CPU times needed for simulation were 8 hours 15 minutes, 7 hours and 6 hours 30 minute for sheet thickness of 1mm, 2mm and 3mm respectively. The peak values of effective strain for 1mm thickness of blank are smaller than those corresponding to 2mm and 3mm thick blank. But a comparison of peak effective strain values for 2mm and 3mm sheet thickness indicates that the values corresponding to 2mm thickness are smaller at initial stages of deformation but become higher with increase of deformation. The punch load increases with increases of punch displacement and thickness of sheet.

8. CONCLUSIONS

A study of adaptive mesh refinement during the sheet stretching operations has been carried out. Three different cases of sheet thickness have been analyzed. The significant conclusions of the present study are summarized below.

1. An initial user-defined mesh is refined automatically whenever the solution error exceeds a predefined limit. It gets finer in places of high gradients of strain rate and coarser in places of low gradients. Therefore, adaptive simulation is well suited to predict seat of large deformation.
2. In sheet stretching operations, two zone of high density mesh are developed. The zone of elements is located away from the centre at lower values of sheet thickness. It moves towards the centre of the blank in the case of higher values of sheet thickness. The finer element zone is wider in the case of lower sheet thickness but becomes localized with increase of

sheet thickness. Also, the finer element zone moves gradually away from the centre of the blank with increase of deformation.

3. The CPU time for process simulation decreases with increase of sheet thickness and the punch load increases with increases of sheet thickness.

9. REFERENCES

1. Cao, H. L. and Teodosiu, C., 1992, "Numerical Simulation Of Drawbeads for Axisymmetric Deep Drawing Processes", Numerical Methods in Industrial Forming, Chenot, et. al. (Eds.), 439-448.
2. Damir, V., 1996, "Flow Formulation FE Metal Forming Analysis with Boundary Friction Via a Penalty Function", J. Mater. Process. Technol., Vol. 59, 272-277.
3. Mark, C. and Julu, M., 2003, “Deep Drawing Process: Analysis and Experiments”, J. Mater. Process. Technol., Vol. 132, 35-41.
4. Zienkiewicz, O. C. and Zhu, J. Z., 1987, “A simple error estimator and adaptive procedure for practical engineering analysis”, Int. J. Num. Meth. Engg.,Vol. 24, pp. 335-357.
5. Zienkiewicz, O. C. and Zhu, J. Z., 1992, “The Superconvergent Patch Recovery and a posteriori Error Estimates, Part I, The Error Recovery Technique”, Int. J. Num. Meth. Engg., Vol. 33, pp. 1331-1364.
6. Singh, D., Sekhon, G. S. and Shishodia, K. S., 1999, “Finite Element Analysis of Metal Forming Processes With Error Estimation and Adaptive Mesh Generation”, Proc. of 11th ISME conf., pp. 616-621.
7. Yoon, J.H. and Huh, H., 2003, “Efficiency Enhancement in Sheet Metal Forming Analysis with a Mesh Regularization Method”, J. Mater. Process. Technol., Vol. 140, 616-621.
8. Kobayashi, S., Oh, S. and Altan T., 1989, Metal forming and the finite element method, Oxford University Press.
9. Li, X. D. and Wiberg, N. E., 1994, “A *posteriori* Error Estimate by Element Patch Post-processing, Adaptive Analysis in Energy and L_2 Norms”, Comp. Struct., Vol. 53, No. 4, pp. 907-919.
10. Garino, C. G. and Oliver, j., 1992, "Use of a large strain elastoplastic model for simulation of metal forming process", Numerical Methods in Industrial Forming, Chenot, et. al. (Eds.), 467-472.

10. NOMENCLATURE

Symbol	Meaning	Unit
$\bar{\sigma}$	effective stress	(Pa)
σ'_{ij}	deviatoric stress tensor	
$\bar{\varepsilon}$	effective strain	
$\dot{\bar{\varepsilon}}$	effective strain rate	(/sec)
ξ , η	natural coordinates	
$\dot{\boldsymbol{\varepsilon}}_v$	volumetric strain rate	(/sec)
$\boldsymbol{\tau}_i$	surface traction stress	(Pa)
K	penalty constant	
μ	equivalent viscosity of the work material	
$\boldsymbol{v}$	velocity vector	
B	strain rate matrix	
D	material matrix	
N	shape function matrix	
N	total number of finite elements in the problem domain Ω	
$\lVert e_i \rVert$	the norm of error in the ith element	